A high-field magnetization study of a $Nd_2Fe_{14}Si_3$ single crystal

2009 J. Phys.: Condens. Matter 21 146005

(http://iopscience.iop.org/0953-8984/21/14/146005)

J. Phys.: Condens. Matter **21** (2009) 146005 (8pp) doi:10.1088/0953-8984/21/14/146005

A high-field magnetization study of a $Nd_2Fe_{14}Si_3$ single crystal

A V Andreev[1,2,7], S Yoshii[3,8], M D Kuz'min[4], F R de Boer[1,2,3,5], K Kindo[6] and M Hagiwara[3]

[1] Joint Laboratory for Magnetic Studies, Institute of Physics, Academy of Sciences, Na Slovance 2, 18221 Prague 8, Czech Republic
[2] Department of Condensed Matter Physics, Charles University, Ke Karlovu 5, 12116 Prague 2, Czech Republic
[3] KYOKUGEN, Osaka University, Toyonaka, Osaka 560-8531, Japan
[4] Leibniz-Institut für Festkörper- und Werkstoffforschung, PF 270116, 01171 Dresden, Germany
[5] Van der Waals-Zeeman Institute, University of Amsterdam, Valckenierstraat 65, 1018 XE Amsterdam, The Netherlands
[6] ISSP, University of Tokyo, 5-1-5 Kashiwanoha, Kashiwa, Chiba 277-8581, Japan

E-mail: andreev@mag.mff.cuni.cz

Received 23 December 2008, in final form 20 February 2009
Published 13 March 2009
Online at stacks.iop.org/JPhysCM/21/146005

Abstract

Magnetization study of a single crystal of $Nd_2Fe_{14}Si_3$ (with the rhombohedral Th_2Zn_{17}-type structure) reveals that the compound is a ferromagnet with a spontaneous magnetic moment of $32.3\mu_B$ per formula unit (at $T = 2$ K) and a Curie temperature equal to 495 K. The easy-magnetization direction lies close to the *b*-axis, tilting slightly towards the *c*-axis. (The *b*-axis [120] is not a high-symmetry direction in the crystallographic class D_{3d}.) The observed strong magnetic anisotropy is attributed almost entirely to the Nd sublattice, as concluded from comparison with a $Y_2Fe_{14}Si_3$ single crystal. A magnetic field applied along the *c*-axis induces a first-order spin reorientation transition at $B_{FOMP} = 20$ T. In the process of magnetization the Nd and Fe sublattices behave as essentially non-collinear. This is manifest particularly in the downward curvature of the first (pre-FOMP) stage of the magnetization curve. It is proposed to regard this curvature as a validity criterion for the single-sublattice approximation.

1. Introduction

The compound $Nd_2Fe_{14}Si_3$, a Si solid solution in the binary intermetallic Nd_2Fe_{17}, belongs to a wide class of rare-earth (R) compounds with a high content of 3d transition metal (T). The R–T intermetallics combine localized magnetism of the R sublattice with itinerant magnetism of the T sublattice [1–3]. This combination makes them very interesting subjects from a scientific point of view. The large magnetic anisotropy and magnetostriction, originating from the R sublattice, in combination with a high spontaneous magnetic moment M_s and Curie temperature T_C, originating from the 3d sublattice, has led to the discovery of several excellent materials for application as permanent magnets and magnetostrictors [4–6].

R_2Fe_{17} is one of widest groups of the R–T intermetallics. The crystal structure of R_2Fe_{17} consists of one (the rhombohedral Th_2Zn_{17}-type in the case of light R) or two (the hexagonal Th_2Ni_{17}-type for heavy R) non-equivalent positions for the R atoms and four positions for the Fe atoms. The compounds are well known for their peculiar magnetic behavior. They have a very short Fe–Fe distance d_{FeFe} between the Fe atoms in one of positions (so-called 'dumbbells'), 239 pm, and several other distances with d_{FeFe} about 244 pm, which are also shorter than the d_{FeFe} about 250 pm in bcc Fe. The short Fe–Fe distances in the 'dumbbells' are expected to give rise to negative exchange interactions. The total Fe–Fe exchange interaction is positive, however, the existence of these competitive interactions leads to remarkably low T_C values for such a high content of Fe. It is interesting that any substitutions in the Fe sublattices, magnetic or non-magnetic, immediately destroy this delicate balance

[7] Author to whom any correspondence should be addressed.
[8] Present address: Institute for Materials Research, Tohoku University, Katahira 2-1-1, Sendai 980-8578, Japan.

of exchange interactions, and T_C increases rapidly. R_2Fe_{17} compounds are also known to possess a large spontaneous magnetostriction. This leads, in combination with the relatively low T_C, to invar behavior in a wide temperature range [1].

Since R_2Fe_{17} compounds exhibit large magnetic anisotropy, single crystals are strongly desirable for quantitative studies of their magnetism. All R_2Fe_{17} compounds with heavy R (except Yb) have been prepared in single-crystalline form and have been studied by many groups [7–9]. As regards the light R compounds, preparation of single crystals looks very difficult due to the complicated phase diagram. Single crystals have been obtained only for Nd_2Fe_{17}. The single crystal was prepared by the flux method and the magnetization was measured in fields up to 6 T [10]. The compound is a ferromagnet with $M_s = 39\mu_B$ per formula unit and $T_C = 348$ K. The magnetic moments are located in the basal plane, the *c*-axis is the hardest magnetization axis. This easy-plane anisotropy is very large, the anisotropy field B_a being estimated to exceed 20 T. Very large anisotropy was also observed within the basal plane, with the [120] axis (the *b*-axis in the orthorhombic coordinates) as the easiest magnetization direction. Later on, the field range of magnetization measurements was extended to 22 T and two field-induced transitions at 10 and 18 T, interpreted as FOMPs (first-order magnetization processes), were observed in the magnetization along the *c*-axis [11]. However, the results obtained on this crystal give rise to some questions. The curve measured along the (easiest) [120] axis (*b*-axis) exhibits a rather high differential magnetization even at the highest field, which may be due to a less-perfect quality of the crystal. Also, the magnetization measured along the [100] axis (*a*-axis) does not approach the *b*-axis curve in high fields. This would correspond to infinitely large anisotropy within the basal plane, which is not realistic. Earlier calculations (open circles in figure 18(a) of [11]) did not reproduce the second magnetization jump. A second magnetization jump observed under similar conditions in Tb_2Fe_{17} was reliably attributed to a secondary phase [12]. In view of these unanswered questions, another study on a new crystal is desirable. However, our attempts to prepare a Nd_2Fe_{17} single crystal by the Czochralski method in a tri-arc furnace have failed, although this method is rather successful in the case of the heavy R compounds. An attempt to grow Nd_2Fe_{17} by the Bridgman method in a Al_2O_3 crucible was successful but, unfortunately the crystal was contaminated by Al, having the composition $Nd_2Fe_{16.3}Al_{0.7}$ [13]. The results of magnetization measurements on this crystal resemble those reported for Nd_2Fe_{17}, including a two-step transition (11.5 and 15 T) along the hard *c*-axis but, in contrast, a spontaneous component of the magnetic moment was observed along this direction that may also point to a less-perfect quality of the crystal. It is known that Si can be substituted for Fe in R_2Fe_{17}, in amounts of up to $x = 3$ according to the formula $R_2Fe_{17-x}Si_x$. A study of polycrystalline $R_2Fe_{14}Si_3$ compounds [14] has revealed a strong modification of the exchange interactions compared to R_2Fe_{17}. In $Nd_2Fe_{14}Si_3$, T_C is reported to be 492 K [14, 15] (compared with 348 K for Nd_2Fe_{17}), whereas M_s decreases. The effect of Si substitution on the magnetic anisotropy of Nd_2Fe_{17} is not known at all because of the lack of any single crystals. We have attempted to grow single crystals of $Nd_2Fe_{17-x}Si_x$ solid solutions by the Czochralski method. This turned out to be impossible for x up to 2.5, but the composition $Nd_2Fe_{14}Si_3$ was found to melt congruently and a crystal could successfully be grown.

In this work, we present the field and temperature dependences of the magnetization measured along the principal axes of the grown $Nd_2Fe_{14}Si_3$ single crystal. Also, the crystals of $R_2Fe_{14}Si_3$, with Y and Ce instead of Nd, were grown and studied to determine the contribution from the Fe sublattice to the magnetic properties.

2. Experimental details

Single crystals of $Nd_2Fe_{14}Si_3$, $Y_2Fe_{14}Si_3$ and $Ce_2Fe_{14}Si_3$ were prepared by arc melting the pure elements (99.9% Nd, Y or Ce, 99.98% Fe and 99.999% silicon) in a tri-arc furnace on a water-cooled copper crucible under a protective argon atmosphere. The alloy buttons were turned several times and then, in order to ensure good homogeneity, kept in the molten state for about 1 h before pulling crystals. The single crystals were grown from these molten buttons by the Czochralski method using a tungsten rod as a seed with 10 mm h^{-1} pulling speed.

The x-ray Laue patterns show that the quality of the crystals is good. The misorientation of subgrains does not exceed 1°. Phase purity and lattice parameters were determined by standard x-ray diffractometry with Cu Kα radiation on powders prepared from the single crystals. $Nd_2Fe_{14}Si_3$ crystallizes in the rhombohedral crystal structure of the Th_2Zn_{17} type (space group $R\bar{3}m$) with lattice parameters $a = 8.519$ Å, $c = 12.470$ Å. $Ce_2Fe_{14}Si_3$ has the same crystal structure with $a = 8.450$ Å, $c = 12.443$ Å. $Y_2Fe_{14}Si_3$ has the hexagonal structure of the Th_2Ni_{17} type (space group $P6_3/mmc$) with $a = 8.419$ Å, $c = 8.284$ Å.

The magnetization curves were measured at 2–600 K along the principal axes of the single crystals using a PPMS-14 magnetometer (Quantum Design) in fields up to 14 T. The magnetization curves presented below are corrected for the demagnetization field. At 4.2 K, the magnetization measurements of $Nd_2Fe_{14}Si_3$ were extended up to 52 T using a non-destructive pulsed-field magnet with a pulse duration of 40 ms installed at the Center for Quantum Science and Technology under Extreme Conditions (KYOKUGEN) at Osaka University. The magnetization was detected by an induction method with a standard pick-up coil system.

3. Results and discussion

3.1. Fe sublattice

Figure 1 shows the magnetization curves of a $Y_2Fe_{14}Si_3$ single crystal at different temperatures. A moderate magnetic anisotropy of the easy-plane type is seen from comparison of the curves at 5 K along the *a* and *c* axes. The spontaneous magnetization, M_s (5 K), equals $26\mu_B$/f.u., which corresponds to an average Fe magnetic moment $M_{Fe} = 1.86\mu_B$. This is

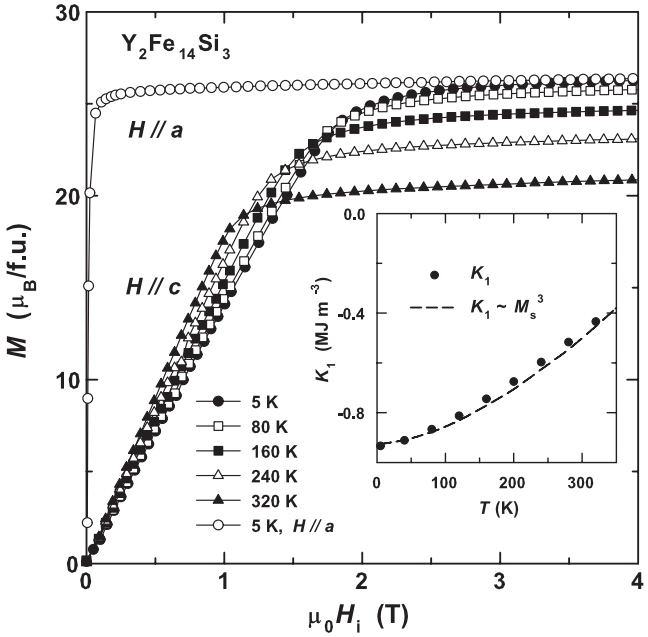

Figure 1. Magnetic isotherms in fields applied along the c-axis of a $Y_2Fe_{14}Si_3$ single crystal. For $T = 5$ K, the curve along the a-axis is shown as well. The inset shows the temperature dependence of K_1, the dashed line representing a fit to $K_1(T) = K_1(0)[M_s(T)/M_s(0)]^3$.

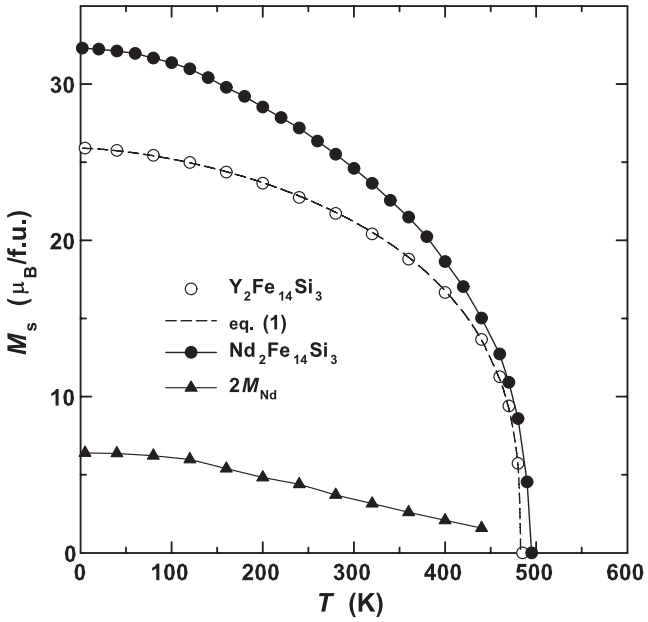

Figure 2. Temperature dependence of M_s for $Y_2Fe_{14}Si_3$ and $Nd_2Fe_{14}Si_3$, as well as the magnetic moment of the Nd sublattice. The dashed line represents the fit of $M_s(T)$ for $Y_2Fe_{14}Si_3$ to equation (1).

significantly less than the Fe moment ($2.05\mu_B$) in the pure Y_2Fe_{17} [16], so that the role of Si cannot be reduced to a mere dilution of the Fe sublattice.

The temperature dependences of M_s for $Y_2Fe_{14}Si_3$ and $Nd_2Fe_{14}Si_3$, obtained from the magnetization isotherms along the easy axis, are presented in figure 2. As shown by the dashed line in figure 2, $M_s(T)$ of $Y_2Fe_{14}Si_3$ is well described by the formula [17]:

$$M_s(T) = M_s(0)\left[1 - 0.8\left(\frac{T}{T_C}\right)^{3/2} - 0.2\left(\frac{T}{T_C}\right)^{5/2}\right]^{1/3} \quad (1)$$

with $M_s(0) = 26.1\mu_B$/f.u. and $T_C = 483$ K. Therefore, to a good approximation $Y_2Fe_{14}Si_3$ can be regarded as a single-sublattice ferromagnet and one can consider it without taking into account four individual Fe sublattices.

The anisotropy field B_a in $Y_2Fe_{14}Si_3$ is equal to 2 T, which is two times smaller than in Y_2Fe_{17}. The good linearity of the hard-direction magnetization curve indicates that the first anisotropy constant K_1 is sufficient to describe the magnetic anisotropy. We refer to the standard expression for the anisotropy energy of hexagonal crystals,

$$E_a = K_1 \sin^2\theta + K_2 \sin^4\theta + K_3 \sin^6\theta + K_3'' \sin^6\theta \cos 6\varphi \quad (2)$$

where θ and φ are the spherical angles defining the direction of the magnetization vector with respect to the crystallographic axes. A Sucksmith–Thompson analysis [18] of the c-axis magnetization curve provides $K_2 = 0.038$ MJ m^{-3}, which can be neglected in comparison with the absolute value of $K_1 = -0.93$ MJ m^{-3}. The sixth-order anisotropy constants K_3 and K_3'' should be all the more negligible. In particular, K_3'' is zero since there is no observable anisotropy within the basal plane, i.e. no difference between the magnetization curves along the [100] (a) and [120] (b) axes.

As can be seen in the inset of figure 1, the temperature dependence of K_1 nicely obeys the relation

$$\frac{K_1(T)}{K_1(0)} = \left[\frac{M_s(T)}{M_s(0)}\right]^3 \quad (3)$$

as follows from the single-ion model in the special case of $|K_1| \gg |K_2|$.

Since $Y_2Fe_{14}Si_3$ and $Nd_2Fe_{14}Si_3$ have different structural modifications, it was necessary to check to what extent such a difference affects the magnetic properties of the Fe sublattice. To this end, we measured magnetization curves of a single crystal of $Ce_2Fe_{14}Si_3$, which has the same rhombohedral structure as $Nd_2Fe_{14}Si_3$. Ce is known to be tetravalent and therefore non-magnetic in Fe-rich intermetallics [1]. No qualitative difference was found between the magnetic properties of $Y_2Fe_{14}Si_3$ and $Ce_2Fe_{14}Si_3$. In particular, $Ce_2Fe_{14}Si_3$ exhibits the same planar magnetic anisotropy with no anisotropy within the easy plane. The spontaneous moment and anisotropy constants in the ground state, $M_s = 25.6\mu_B$/f.u., $K_1 = -0.90$ MJ m^{-3}, $K_2 = 0.05$ MJ m^{-3}, are practically the same as in $Y_2Fe_{14}Si_3$. The $K_1(T)$ dependence follows equation (3) as well. Moreover, very similar results were also obtained on $Lu_2Fe_{14}Si_3$ with non-magnetic Lu (the hexagonal structure with considerably smaller lattice parameters, $a = 8.361$ Å, $c = 8.295$ Å due to the smaller atomic radius of Lu) [19].

Thus, to a good approximation, $R_2Fe_{14}Si_3$ with non-magnetic R can be regarded as single-sublattice ferromagnets with magnetic anisotropy of the easy-plane type, i.e. they

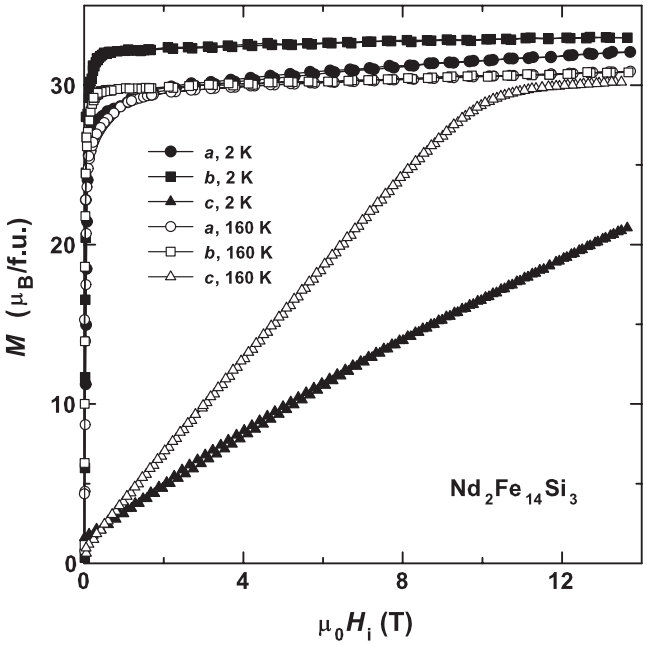

Figure 3. Magnetization isotherms in steady fields applied along the principal axes of a $Nd_2Fe_{14}Si_3$ single crystal at 2 and 160 K.

can be treated without taking into account four individual Fe sublattices. The magnetic properties of all such compounds are rather similar, irrespective of structure modifications, different atomic radii or effective valence of R.

3.2. Anisotropy constants of $Nd_2Fe_{14}Si_3$ as obtained by the Sucksmith–Thompson method

Figure 3 displays magnetization curves along the principal axes of the $Nd_2Fe_{14}Si_3$ single crystal at a low temperature (2 K) and at a representative elevated temperature of 160 K. The curves reveal large magnetic anisotropy of an easy-plane type with the *b*-axis as the easy-magnetization direction, which is qualitatively the same as in Nd_2Fe_{17}. Details of the temperature evolution of the magnetization curves along the *c*-axis and within the basal plane are presented in figures 4 and 5, respectively. $Nd_2Fe_{14}Si_3$ is ferromagnetic below $T_C = 495$ K and $M_s = 32.3\mu_B$/f.u. in the ground state. The magnetic moment per Nd atom, obtained from the difference between M_s of $Nd_2Fe_{14}Si_3$ and $Y_2Fe_{14}Si_3$, is $M_{Nd} = 3.2\mu_B$, which is close to the moment of the single Nd^{3+}-ion.

Above 120 K, the *c*-axis curves are practically linear (which indicates a good quality of the crystal) and they saturate in a continuous fashion below the maximum available field of 14 T. Therefore, we applied the Sucksmith–Thompson method to determine the anisotropy constants of the compound. Generally the method cannot be used for ferromagnets with the rhombohedral Th_2Zn_{17} structure, even if the six-order anisotropy terms are small. The reason is an extra fourth-order term appearing in the expression for the anisotropy energy appropriate for the symmetry class D_{3d},

$$E_a = K_1 \sin^2\theta + K_2 \sin^4\theta + K_2' \sin^3\theta \cos\theta \sin 3\varphi + K_3 \sin^6\theta + K_3' \sin^3\theta \cos\theta (11\cos^2\theta - 3) \sin 3\varphi + K_3'' \sin^6\theta \cos 6\varphi. \quad (4)$$

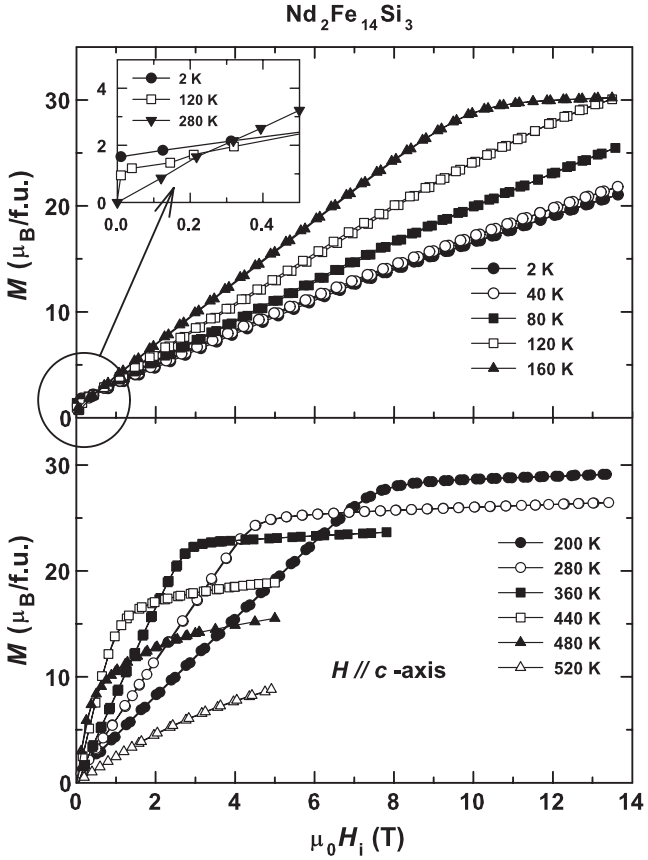

Figure 4. Temperature evolution of the magnetization curve along the *c*-axis of $Nd_2Fe_{14}Si_3$.

The *x*-axis (*a*) has been set along a two-fold symmetry axis, as recommended by the International Tables for Crystallography. Hence the use of $\sin 3\varphi$ in equation (4) instead of the more usual $\cos 3\varphi$. There are six easy-magnetization directions oriented as follows: $\varphi = -\pi/6 + n\pi/3$, $\theta = \pi/2 + (-1)^n\delta$, $n = 1, 2, \ldots, 6$. Similar non-coplanar easy-star structures have already been observed in the isomorphous Nd_2Co_{17} and Pr_2Co_{17} compounds, with $\delta = 8°$ and 26°, respectively [20, 21].

The peculiarity of $Nd_2Fe_{14}Si_3$ is that the deviation of the easy directions from the basal plane is rather small, $\delta \approx 3°$ at $T = 4.2$ K, as determined from the initial part of the magnetization curve along the *c*-axis, figure 4. The angle δ decreases with temperature, becoming indiscernible above 250 K (figure 6). For δ small, one has

$$\delta = \frac{K_2' - 3K_3'}{2K_1 + 4K_2 + 6(K_3 - K_3'')}. \quad (5)$$

In a situation when the sixth-order anisotropy constants can be neglected, the smallness of δ provides grounds for neglecting K_2' as well. Left with the first two anisotropy terms in equation (4), we were able to use the Sucksmith–Thompson technique to determine K_1 and K_2. The results are presented in figure 7. The agreement between the values of the anisotropy constants K_1 and K_2 derived from the steady-field and pulsed-field

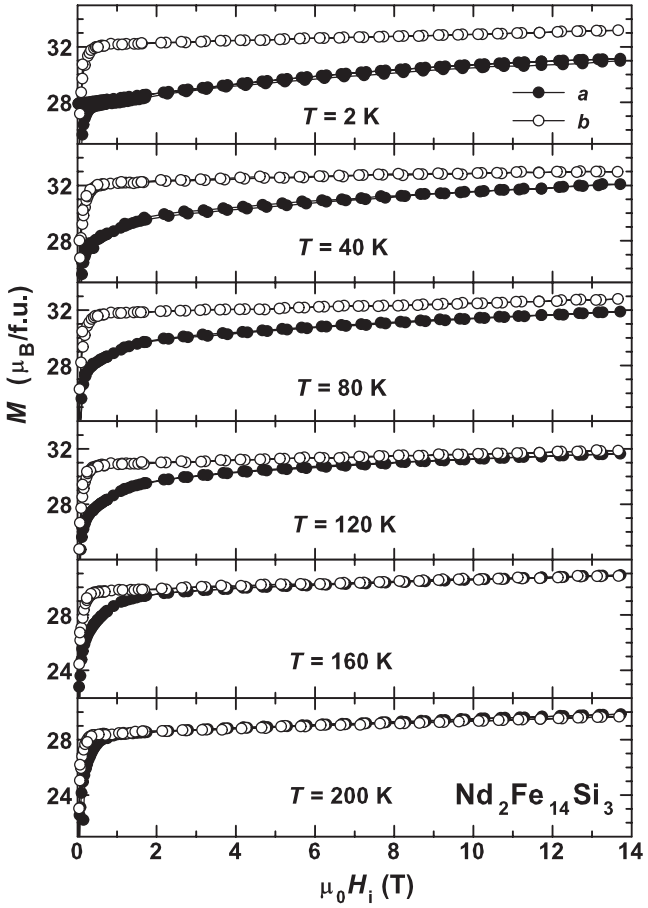

Figure 5. Temperature evolution of the magnetization curves along the a and b axes of $Nd_2Fe_{14}Si_3$.

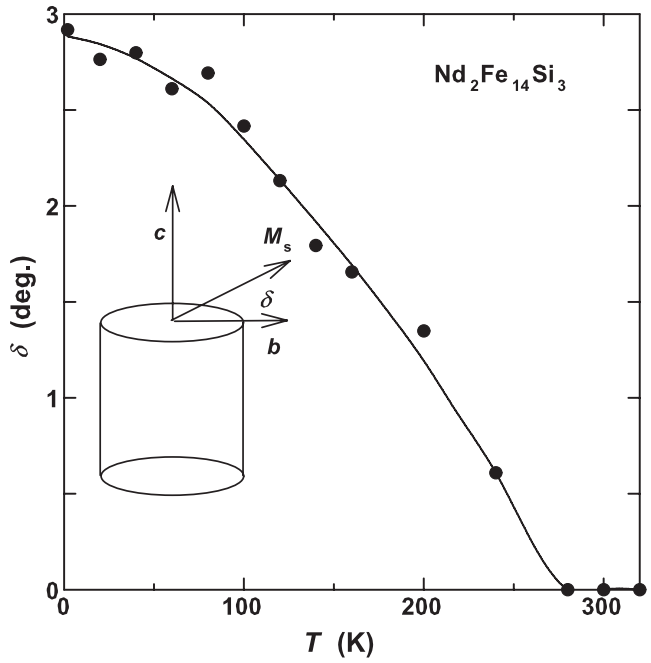

Figure 6. Temperature dependence of the angle δ between M_s and the b-axis.

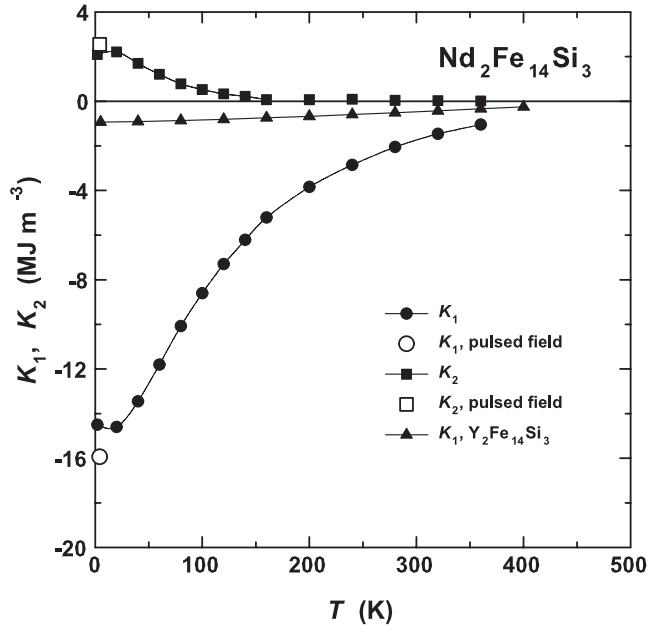

Figure 7. Temperature dependence of K_1 and K_2 of $Nd_2Fe_{14}Si_3$, obtained by the Sucksmith–Thompson method from magnetization curves in steady fields up to 14 T. The open symbols correspond to results of measurements in pulsed fields below FOMP. The triangles represent $K_1(T)$ of $Y_2Fe_{14}Si_3$ (the Fe sublattice).

magnetization is quite satisfactory, the latter values being slightly (about 10%) larger than the values obtained in steady fields. The somewhat larger pulsed-field values (empty symbols in figure 7) can be considered as more reliable because, at lower fields, the influence on the magnetization of imperfectness of crystal or misorientation is relatively larger than in the higher pulsed fields. In the ground state, $Nd_2Fe_{14}Si_3$ is characterized by $K_1 = -15$ MJ m^{-3}. This splits between $K_{1Nd} = -14$ MJ m^{-3} (-260 K/f.u.) and $K_{1Fe} = -1$ MJ m^{-3}, i.e. $|K_{1Nd}| \gg |K_{1Fe}|$. The second anisotropy constant, $K_2 = 2$ MJ m^{-3}, can be attributed entirely to the Nd sublattice, because K_{2Fe} is only 0.04 MJ m^{-3}.

The obtained values of K_{1Nd} and K_{2Nd} look reasonable, but if we compare $K_{1Nd}(T)$ with $M_{Nd}(T)$, the observed K_{1Nd} decreases much faster with temperature than expected from equation (3). The derived temperature dependence of K_{1Nd} poses some doubt on the applicability of the Sucksmith–Thompson method to the c-axis magnetization curve of $Nd_2Fe_{14}Si_3$ at low temperatures. This is also demonstrated when we consider the magnetization curves along the principal axes at 4.2 K in higher fields up to 52 T (figure 8). The occurrence of a FOMP transition around 20 T in the magnetization along the c-axis cannot be accounted for by a positive value of K_2 as obtained in the Sucksmith–Thompson analysis.

The six-fold anisotropy constant K_3'' describing the anisotropy within the easy plane is equal to 1.9 MJ m^{-3} (35 K/f.u.) at 2 K and very rapidly decreases with increasing temperature (figure 5). (Since K_3'' is proportional to the relatively small area between the magnetization curves along the a and b axes, the experimental error is about 30%.)

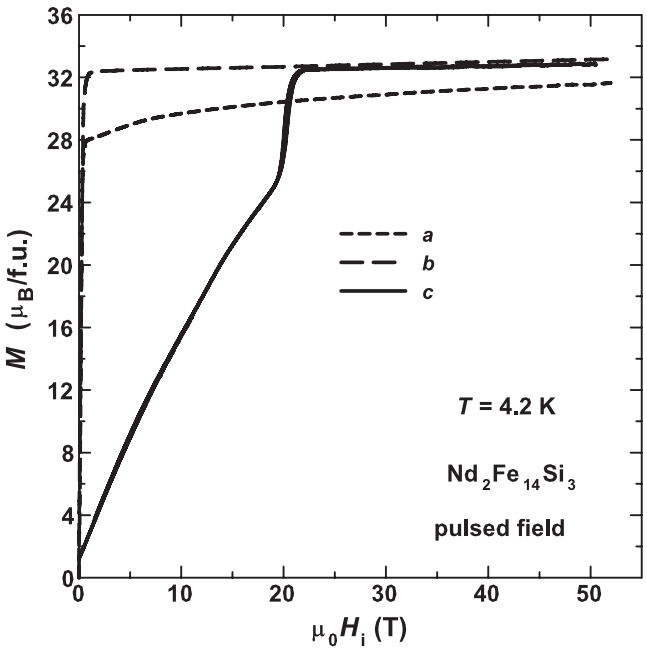

Figure 8. Magnetization curves along the principal axes of $Nd_2Fe_{14}Si_3$, measured in pulsed fields at 4.2 K.

3.3. The two-sublattice model

In section 3.2 $Nd_2Fe_{14}Si_3$ was regarded as a one-sublattice ferromagnet. The physical approximation underlying the notion of perfectly parallel Fe and Nd sublattices—that of an Fe–Nd exchange much stronger than the anisotropy—apparently fails for $Nd_2Fe_{14}Si_3$. A manifestation of this failure was our inability to describe the magnetization curve along the *c*-axis, which features a FOMP, using a single set of anisotropy constants. In this section we refine our approach by allowing for two non-collinear magnetic sublattices—a single combined Fe sublattice and a sublattice of Nd. We consider the following (non-equilibrium) thermodynamic potential:

$$\Phi(\mathbf{M}_{\mathrm{Fe}}, \mathbf{M}_{\mathrm{Nd}}, \mathbf{B}) = -\lambda \mathbf{M}_{\mathrm{Fe}} \cdot \mathbf{M}_{\mathrm{Nd}} - (\mathbf{M}_{\mathrm{Fe}} + \mathbf{M}_{\mathrm{Nd}}) \cdot \mathbf{B} + E_{\mathrm{a}}^{\mathrm{Fe}} + E_{\mathrm{a}}^{\mathrm{Nd}}. \quad (6)$$

Here the first term describes the Fe–Nd exchange, while the second one describes the interaction with the applied magnetic field. The last two terms are anisotropy energies of the two sublattices. Our consideration is limited to low temperatures, so we assume $|\mathbf{M}_{\mathrm{Fe}}| = M_{\mathrm{Fe}} = \text{const.}$ and $|\mathbf{M}_{\mathrm{Nd}}| = M_{\mathrm{Nd}} = \text{const.}$

A specific description of the magnetization process depends on the direction of the applied magnetic field. We shall consider in detail the simplest case, $\mathbf{B}||[001]$ (*c*-axis). In the case of $Nd_2Fe_{14}Si_3$ (easy direction close to [120]) the three vectors, $\mathbf{M}_{\mathrm{Fe}}$, $\mathbf{M}_{\mathrm{Nd}}$ and $\mathbf{B}$, will lie in one of the {110} planes. The orientation of $\mathbf{M}_{\mathrm{Fe}}$ and $\mathbf{M}_{\mathrm{Nd}}$ can be described by the angles they make with $\mathbf{B}$, α and β, respectively. The thermodynamic potential takes the following form:

$$\Phi(\alpha, \beta) = -\lambda M_{\mathrm{Fe}} M_{\mathrm{Nd}} \cos(\alpha - \beta) - M_{\mathrm{Fe}} B \cos\alpha - M_{\mathrm{Nd}} B \cos\beta + K_{1\mathrm{Nd}} \sin^2\beta + K_{2\mathrm{Nd}} \sin^4\beta. \quad (7)$$

The last terms stand for the anisotropy energy of the Nd sublattice. The anisotropy energy of the Fe sublattice is much smaller and has been left out. The equilibrium orientation of the sublattice vectors is found by minimizing equation (7) with respect to α and β. To this end it is convenient to introduce dimensionless variables. Let us express all the energies in the units of $\lambda M_{\mathrm{Fe}}^2$; thus $\phi = \Phi/\lambda M_{\mathrm{Fe}}^2$ is the dimensionless thermodynamic potential and $\kappa_1 = K_{1\mathrm{Nd}}/\lambda M_{\mathrm{Fe}}^2 < 0$ and $\kappa_2 = K_{2\mathrm{Nd}}/\lambda M_{\mathrm{Fe}}^2 < 0$ are dimensionless anisotropy constants. The magnetic field should be related to the molecular field on the R sublattice, $b = B/\lambda M_{\mathrm{Fe}}$. Finally, all magnetizations are referred to the larger one of the sublattice magnetizations, which is M_{Fe}. According to this convention, the magnetization of the iron sublattice is unity, while that of the rare-earth sublattice equals $m = M_{\mathrm{Nd}}/M_{\mathrm{Fe}}$, $0 \leqslant m \leqslant 1$. Using the dimensionless variables, the thermodynamic potential (7) is rewritten as follows:

$$\phi(\alpha, \beta) = -m\cos(\alpha - \beta) - b\cos\alpha - mb\cos\beta + \kappa_1 \sin^2\beta + \kappa_2 \sin^4\beta. \quad (8)$$

The reduced total magnetization in the direction of the applied magnetic field is given by

$$\sigma = \frac{\cos\alpha + m\cos\beta}{1 + m} \quad (9)$$

where α and β are the equilibrium values of the sublattice orientation angles, obtained by minimizing equation (8). Since the minimization cannot be carried out analytically, we shall proceed as follows. First, equation (8) is minimized with respect to α, which results in

$$m\sin(\alpha - \beta) + b\sin\alpha = 0 \quad (10)$$

or

$$\alpha = \arctan\frac{m\sin\beta}{b + m\cos\beta}. \quad (11)$$

This expression can be used to eliminate α from the minimization procedure. Now the function $\phi(\alpha(\beta), \beta)$ needs to be minimized with respect to just one variable β. This is carried out by trial and error, taking for β, values between 0 and $\pi/2$ in increments of 0.001.

Our goal is to find the unknown parameters κ_1 and κ_2 corresponding to the experimentally observed shape of the low-temperature magnetization curve of $Nd_2Fe_{14}Si_3$ with $\mathbf{B}||[001]$. Note that the parameter m is known: $m = 6.5/26 = 0.25$. To facilitate the comparison of the shape of the curves with different κ_1 and κ_2, it is convenient to bring all the curves to the same scale. To this end, the computed reduced magnetization is plotted against a rescaled abscissa, b/b_{FOMP} or B/B_{FOMP}, see figure 9. The curves to compare then lie within the unitary square.

Further, we are only interested in such curves whose critical reduced magnetization corresponds to the value observed experimentally, $\sigma_{\mathrm{cr}} = 0.77$. This restriction defines a curve in the plane of the parameters κ_1 and κ_2, figure 10. (The construction of this curve is straightforward: for each chosen κ_2, κ_1 is varied until the condition $\sigma_{\mathrm{cr}} = 0.77$ is fulfilled.) Some representative $\sigma(B/B_{\mathrm{FOMP}})$ dependences are displayed

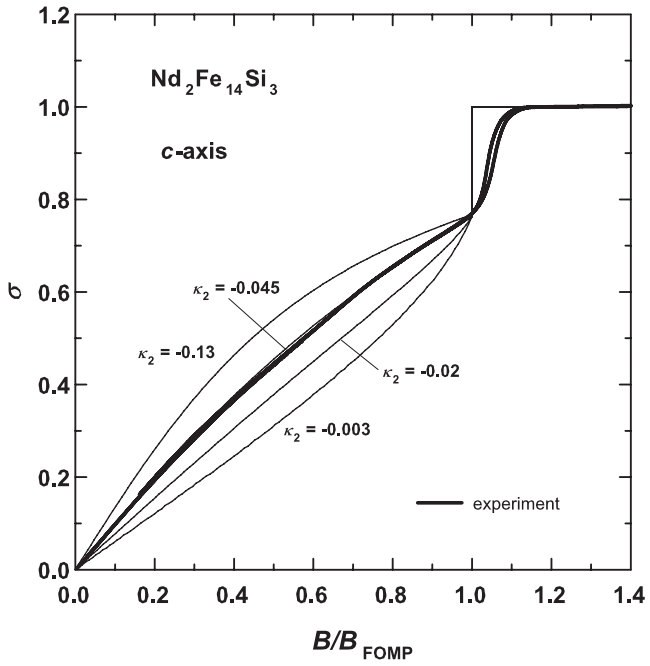

Figure 9. Reduced magnetization versus reduced magnetic field applied along the c-axis. Bold line: experimental data upon deducting the projection of the spontaneous magnetization. Thin lines: calculations using κ_2 indicated on the curves and κ_1 determined from the condition $\sigma_{cr} = 0.77$.

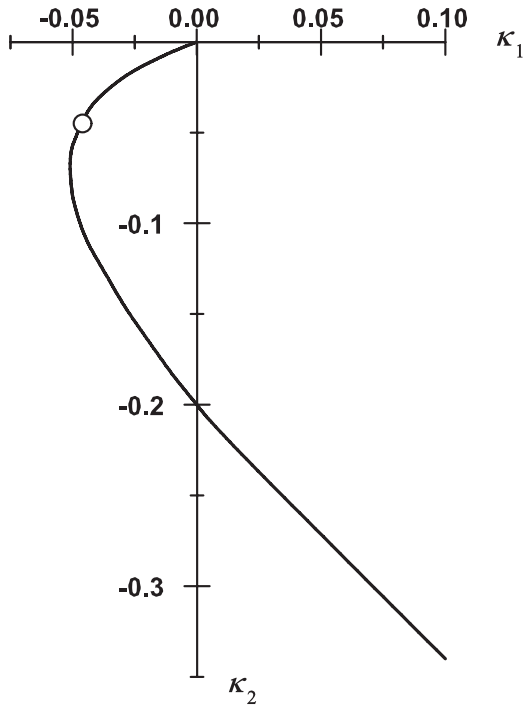

Figure 10. Solid curve: set of points (κ_1, κ_2) satisfying the condition $\sigma_{cr} = 0.77$. Open circle: the best-fit (κ_1, κ_2) for $Nd_2Fe_{14}Si_3$.

in figure 9. One can appreciate that both the magnitude, and the sign of the curvature, change according as the locus of the point (κ_1, κ_2) moves along the line drawn in figure 10.

In the weakly anisotropic limit, when (κ_1, κ_2) lies near the origin in figure 10, the magnetization isotherms are curved upwards. Here the non-collinearity of the sublattices can be neglected and the system is equivalent to a single-sublattice ferromagnet. The presence of a FOMP requires that $\kappa_2 < 0$, which then means an upward curvature for the magnetization. One could use the Sucksmith–Thompson technique to determine the anisotropy constants in this region. We note that the initial slope of the curve in figure 10 is determined by the critical magnetization σ_{cr} alone and equals $(1 + \sigma_{cr})^{-1}(3\sigma_{cr} - 1)^{-1} \approx 0.43$, cf. equation (7) of [12].

According as the point (κ_1, κ_2) moves away from the origin in figure 10, the field dependences of magnetization gradually acquire a downward curvature, even though κ_2 remains negative. The line in the κ_1–κ_2 plane deviates from its initial course, bends over to the right and eventually leaves the third quadrant for the fourth one. The change of sign of κ_1 is not accompanied by any qualitative change in the magnetization curves, since no phase transition takes place at this point. Quantitatively, the gradual growth of the downward curvature continues as the locus of (κ_1, κ_2) goes to infinity in the fourth quadrant.

The best agreement with experiment is obtained for $\kappa_1 = -0.048$ and $\kappa_2 = -0.045$ (second curve from above in figure 9). This point is indicated with an open circle in figure 10. The corresponding dimensionless threshold field is $b_{FOMP} = 0.13$. Comparing this with the experimental value, $B_{FOMP} = 20$ T, we get for the molecular field on Nd: $B_{mol} = \lambda M_{Fe} = B_{FOMP}/b_{FOMP} = 154$ T. The anisotropy constants of the Nd sublattice are evaluated as follows: $K_{1Nd} = \lambda M_{Fe}^2 \kappa_1 = -7$ MJ m^{-3} and $K_{2Nd} = \lambda M_{Fe}^2 \kappa_2 = 6.5$ MJ m^{-3}. Since this is nearly an order of magnitude larger than $K_{1Fe} = -1$ MJ m^{-3}, the neglect of the latter in our model is *a posteriori* justified.

4. Concluding remarks

It is edifying to compare the low-temperature values of anisotropy constants obtained for $Nd_2Fe_{14}Si_3$ in the one- and two-sublattice models. In the former case we found $K_1 = -15$ MJ m^{-3} and $K_2 = 2$ MJ m^{-3}. These values were deduced by the Sucksmith–Thompson technique from the low-field ($\mu_0 H < 18$ T) part of the magnetization curve along the c-axis. Both K_1 and K_2 are attributable predominantly to the Nd sublattice (even though it is of no great importance how the anisotropy is apportioned among the sublattices assumed collinear). It is essential, however, that the observed FOPM cannot be reproduced in this approach.

Having allowed for non-collinearity of the Nd and Fe sublattices, we got very different anisotropy constants: $K_1 = -7$ MJ m^{-3} and $K_2 = -6.5$ MJ m^{-3}. In order to keep the model simple, we had made a not unreasonable assumption that both anisotropy constants pertain to the Nd sublattice, while the Fe sublattice is magnetically isotropic. Within this approach that FOMP is described rather well. Hence we conclude that the single-sublattice approximation is unapplicable to $Nd_2Fe_{14}Si_3$. The anisotropy constants obtained in that approximation are wrong.

It is an old news that the single-sublattice approximation may fail despite the smallness of the anisotropy-to-(intersublattice) exchange ratio [22]. In order for the

approximation to be valid, this ratio should not just be small as compared with unity but very small. In our study we, too, find that the single-sublattice approximation holds rather well for $\kappa_1 \sim -0.01$, but fails irreparably for $\kappa_1 \sim -0.05$. The difficulty of deciding whether the single-sublattice approximation may be used is exacerbated by the fact that the anisotropy-to-exchange ratio is not known *a priori* with any degree of precision.

More telling than any other parameters is the curvature of the pre-FOMP part of the magnetization versus field dependence. The magnetization curve that features a type-I FOMP and is curved upwards on approach to the anomaly should be tractable within the single-sublattice approximation. Such FOMPs usually take place in relatively weak fields. Typical examples are $U_2Fe_{13.6}Si_{3.4}$ [23] and Tb_2Fe_{17} [12] with $B_{FOMP} \sim 3$ T.

If M versus H has a downward curvature on approach to a type-I FOMP, non-collinearity of the sublattices must be taken into account. These are usually higher-field FOMPs. A paradigm is $NdCo_5$ with $B_{FOMP} = 34$ T [24]. The system studied in this work falls under this category as well.

Unfortunately, we cannot quantitatively compare the results on $Nd_2Fe_{14}Si_3$ (our work) and on Nd_2Fe_{17} (from literature), and thus distinguish the effect of Si substitution, because the data reported on Nd_2Fe_{17} have been obtained on an imperfect crystal and are not very reliable. However, the paper is not particularly devoted to studying the effect of Si substitution on the magnetism of Nd_2Fe_{17} but rather to the behavior of Nd ions in a high-Fe-content matrix. The complicated metallurgy of Nd_2Fe_{17} does not allow us to prepare a single crystal of proper quality and we found that Si substitution is a way to avoid this difficulty. Because we have prepared analogous single crystals with non-magnetic R, we can properly distinguish the Nd contribution to the magnetic properties.

Acknowledgments

This work is a part of the research project AVOZ10100520 and has been supported by grant GACR 202/09/0339. Theoretical work at IFW Dresden was financially supported by Deutsche Forschungsgemeinschaft under the Project RI 932/4-1.

References

[1] Franse J J M and Radwanski R 1993 *Handbook of Magnetic Materials* vol 7, ed K H J Buschow (Amsterdam: North-Holland) p 307
[2] Kuz'min M D and Tishin A M 2008 *Handbook of Magnetic Materials* vol 17, ed K H J Buschow (Amsterdam: North-Holland) p 149
[3] Li H S and Coey J M D 1991 *Handbook of Magnetic Materials* vol 6, ed K H J Buschow (Amsterdam: North-Holland) p 1
[4] Buschow K H J 1997 *Handbook of Magnetic Materials* vol 10, ed K H J Buschow (Amsterdam: North-Holland) p 463
[5] Herbst J F 1991 *Rev. Mod. Phys.* **63** 819
[6] Engdahl G (ed) 2000 *Handbook of Giant Magnetostrictive Materials* (San Diego, CA: Academic) p 409
[7] Andreev A V, Deryagin A V, Zadvorkin S M, Kudrevatykh N V, Moskalev V N, Levitin R Z, Popov Y F and Yumaguzhin R Y 1985 *Fizika Magnitnykh Materialov* (*Physics of Magnetic Materials*) ed D D Mishin, Kalinin University, pp 21–49 (In Russian)
[8] Sinnema S 1988 *PhD Thesis* University of Amsterdam
[9] García-Landa B, Algarabel P A, Ibarra M R, Kayzel F E and Franse J J M 1997 *Phys. Rev.* B **55** 8313
[10] Koyama K, Fujii H and Canfield P C 1996 *Physica* B **226** 363
[11] Koyama K and Fujii H 2000 *Phys. Rev.* B **61** 9475
[12] Kuz'min M D, Skourski Y, Skokov K P, Müller K-H and Gutfleisch O 2008 *Phys. Rev.* B **77** 132411
[13] Koide T, Kato H, Shiomi J, Iriyama T and Yamada M 1995 *J. Magn. Magn. Mater.* **140–144** 983
[14] Shen B G, Liang B, Cheng Z H, Gong T Y, Tang H, de Boer F R and Buschow K H J 1997 *Solid State Commun.* **103** 71
[15] Long G J, Marasinghe G K, Mishra S, Pringle O A, Grandjean F, Buschow K H J, Middleton D P, Yelon W B, Pourarian F and Isnard O 1993 *Solid State Commun.* **88** 761
[16] Prokhnenko O, Kamarád J, Prokeš K, Arnold Z and Andreev A V 2005 *Phys. Rev. Lett.* **94** 107201
[17] Kuz'min M D 2005 *Phys. Rev. Lett.* **94** 107204
[18] Sucksmith W and Thompson J E 1954 *Proc. R. Soc.* **225** 362
[19] Andreev A V, Rafaja D, Kamarad J, Arnold Z, Homma Y and Shiokawa Y 2004 *J. Alloys Compounds* **383** 40
[20] Kudrevatykh N V, Deryagin A V, Kazakov A A, Reimer V A and Moskalev V N 1978 *Phys. Met. Metallogr.* **45** 38
[21] Verhoef R, Franse J J M, de Boer F R, Heerooms H J M, Matthaei B and Sinnema S 1988 *IEEE Trans. Magn.* **24** 1948
[22] Sarkis A and Callen E 1982 *Phys. Rev.* B **26** 3870
[23] Andreev A V, Kolomiets A V and Goto T 2005 *J. Alloys Compounds* **387** 60
[24] Bartashevich M I, Goto T, Yamaguchi M, Yamamoto I and Radwanski R 1993 *Solid State Commun.* **87** 1093